End-Permian extinction amplified by plume-induced release of recycled lithospheric volatiles

DOI:
10.1038/s41561-018-0215-4

Document Version
Accepted author manuscript

End-Permian extinction amplified by plume-induced release of recycled lithospheric volatiles

Michael W. Broadley[1†]; Peter H. Barry[3]; Chris J. Ballentine[3]; Lawrence A. Taylor[4]; Ray Burgess[1]

[1] *School of Earth and Environmental Sciences, The University of Manchester, Manchester M13 9PL, UK*

[3] *Department of Earth Sciences, University of Oxford, Oxford, OX1 3AN, UK*

[4] *Department of Earth and Planetary Science, The University of Tennessee, Knoxville, TN 37996-1410, USA*

[†] Present address: *Centre de Recherches Pétrographiques et Géochimiques, 54501 Vandoeuvre-Lès-Nancy Cedex, France*

Magmatic volatile release to the atmosphere can lead to climatic changes and significant environmental degradation including the production of acid rain, ocean acidification and ozone depletion, potentially resulting in collapse of the biosphere. The largest recorded mass extinction in Earth's history occurred at the end-Permian, coinciding with the emplacement of the Siberian large igneous province, suggesting that large-scale magmatism is a key driver of global environmental change. However, the source and nature of volatiles in the Siberian large igneous province remain contentious. Here we present halogen compositions of sub-continental lithospheric mantle xenoliths emplaced prior to, and after the eruption of the Siberian flood basalts. We show that the Siberian lithosphere is massively enriched in halogens from the infiltration of subducted seawater-derived volatiles and that a significant amount (up to 70%) of lithospheric halogens are assimilated into the plume and released to the atmosphere during emplacement. Plume-lithosphere interaction is therefore a key process controlling the volatile content of large igneous provinces and as such the extent of environmental crises, leading to mass extinctions during their emplacement.

Large igneous provinces (LIP) are the product of rapid eruptions of large volumes of magma over short geological time scales. The Permo-Triassic Siberian flood basalts (SFB) erupted ~4×10^6 km^3 of basalt in less than 1 Ma[1]. The eruption of the SFB is contemporaneous with the main stage of the end-Permian crisis and is hypothesized to have contributed to environmental changes that resulted in loss of >90% of all marine, and >70% of all terrestrial species[2,3]. The end-Permian mass extinction has been attributed to sharp fluctuations in global temperatures and/or increased levels

of ultraviolet radiation resulting from extensive ozone depletion both of which are associated with the magmatic release of volatiles to the atmosphere[2,4-7]. Yet the amount of volatiles expected to be released from the SFB assuming conventional plume source magmatism is insufficient to account for the environmental degradation and climatic fluctuations that occurred during the end-Permian crisis, requiring an additional source of volatiles to be released during SFB emplacement[8,9]. To reconcile the missing SFB volatiles, it has been variously argued for significant quantities of volatiles released via contact metamorphism of a sedimentary sequence[1,5]; melting of recycled eclogite within the mantle plume[10]; or melting of the cratonic lithosphere[7]. However, the source of volatile species responsible for climatic fluctuations and ozone depletion during the end-Permian crisis remains unknown.

Here we report the first detailed halogen (Cl, Br and I) data for peridotite xenoliths from two Siberian kimberlites: one (Udachnaya, 360 Ma) emplaced before, and the other (Obnazhennaya, 160 Ma) after the SFB eruption ~250 Ma[11,12] (Supplementary Fig. 1). The Udachnaya peridotite xenoliths (n=9) represent melt extraction from the depleted cratonic mantle; whereas Obnazhennaya xenoliths (n=6) contain both Archean cratonic lithosphere and melt residues generated from the SFB plume (Supplementary Information)[13]. Determining the halogen composition of the cratonic sub-continental lithospheric mantle (SCLM; Udachnaya) and the SFB plume residues (Obnazhennaya) provides a means to estimate the composition of the SFB prior to eruption, and quantify the contribution of the lithospheric mantle to the halogen budget of the SFB.

Lithospheric mantle as a reservoir for halogens

Due to its isolation and non-convective nature, the SCLM retains geochemical heterogeneities introduced through interactions with mantle, crustal and subduction-related sources[14,15]. Metasomatic components infiltrating the SCLM are sampled by mantle xenoliths. Rapidly transported to the surface during kimberlite volcanism, these xenoliths provide a window into the composition and origin of SCLM volatiles[16-18].

The halogen and noble gas composition of the Udachnaya and Obnazhennaya xenoliths was determined using neutron-irradiated noble gas mass spectrometry (Methods). The results are summarised in Supplementary Tables 2 and 3 and displayed in Fig. 1. The range of Cl, Br and I concentrations within the Udachnaya and Obnazhennaya xenoliths are significantly different, with the average concentrations from crushing and step heating being consistently higher in Udachnaya samples indicating they originate from distinct domains within the SCLM (Supplementary Information). Halogen-bearing fluids present in the samples, as indicated by release during crushing experiments, have a similar range of Br/Cl and I/Cl in both Udachnaya and Obnazhennaya xenoliths (Fig. 2a). During stepped-heating of crushed residues the xenoliths show evidence for distinct endmember halogen compositions (Fig. 2b). Udachnaya retains similar Br/Cl and I/Cl as measured during crushing, whilst Obnazhennaya samples have more mantle-like Br/Cl and I/Cl values (Table S3).

Previously published helium isotopic data also varies between the xenoliths suites, with the average $^{3}He/^{4}He$ of Udachnaya (0.4 ± 0.3 R_A) consistently lower than Obnazhennaya (4.2 ± 0.9 R_A), which has a maximum $^{3}He/^{4}He$ (8.4 ± 0.3 R_A) similar to mid ocean ridge basalts (MORB)[18]. $^{3}He/^{4}He$, Br/Cl and I/Cl values appear to be coupled (Fig. 3), showing that fluids within the Obnazhennaya xenoliths represent a mixture between a component rich in radiogenic ^{4}He, Br and I, and a component with mantle-like $^{3}He/^{4}He$ and halogen compositions. The lower $^{3}He/^{4}He$ and elevated Br/Cl and I/Cl as characterised by Udachnaya xenoliths, is considered representative of the ancient metasomatised section of the SCLM (metasomes) that was present before significant influence of the SFB mantle plume. In contrast, Obnazhennaya also contains variable amounts of a mantle-like halogen and He component. Given the similarity in rare earth elements (REE) patterns and extraction age for the Obnazhennaya xenoliths with regards to the SFB[13], it is considered that mantle-like volatiles were added by the Siberian plume which interacted with the lithosphere having a volatile composition characterised by fluids trapped in the Udachnaya xenoliths (Fig. 3).

The initial inventory of halogens within the metasomatised section of Siberian SCLM prior to plume impingement can be estimated using the composition of Udachnaya xenoliths. The Siberian SCLM transitions from depleted harzburgite and lherzolites to predominantly metasomatised peridotites at 180-190 km[19]. Assuming that the Udachnaya peridotite xenoliths are representative of metasomatised peridotites in the lower 30 km of the SCLM, and taking the surficial area of the Siberian Craton ($4x10^{6}$ km^{2}), then the metasomatised portion of the Siberian SCLM contains approximately $0.6\text{-}1.5\times10^{19}$, $1.6\text{-}2.7\times10^{17}$ and $0.5\text{-}1.1\times10^{14}$ kg of Cl, Br and I

112 respectively (Supplementary Table 1 and Supplementary Information). The
113 metasomatised Siberian SCLM is therefore enriched in Cl, Br and I by factors of up
114 to 125, 675 and 100 times, respectively, relative to the depleted MORB mantle
115 (DMM)[20]. Thus, the SCLM is a significantly larger and more heterogeneous halogen
116 reservoir than previously considered and may impart a significant influence on global
117 volatile cycles[21].

118

119 **Release of lithospheric halogens during LIP emplacement**

120 The comparatively large quantity of halogens residing in the base of the Siberian
121 SCLM means that even small proportions released to the surface will have
122 significant consequences for the global halogen cycle. The eruption of halogens into
123 the stratosphere catalyses ozone-destroying reactions, raising surface levels of
124 biologically damaging UV radiation[22,23]. Transit of the SFB plume through the SCLM
125 could potentially have liberated significant amounts of halogens and other volatiles to
126 the atmosphere, contributing to species decline and extinction during the end-
127 Permian crisis.

128

129 Udachnaya xenoliths formed at significantly deeper depths (>50km difference)[17] in
130 the lithosphere compared to Obnazhennaya. The identification of Udachnaya-like
131 metasomatic signatures in Obnazhennaya indicates that volatiles residing in the
132 metasomatised basal SCLM were mobilised and ascended to shallower parts of the
133 SCLM. Obnazhennaya xenoliths have trace element signatures within the range of
134 previously reported values of the SFB[17], strong P-PGE depletions uncharacteristic of

cratonic lithosphere and Os isotopic compositions consistent with a formation age similar to the time of plume impingement[13]. These characteristics indicate that the part of the lithosphere sampled by the Obnazhennaya kimberlite represents the melt residue of the SFB-plume (Fig. 4d)[13]. The identification of metasomatised SCLM signatures within the Obnazhennaya xenoliths therefore suggests that as the SFB plume impacted the base of the lithosphere, the resulting melts incorporated volatiles mobilised from the deeper metasomatised SCLM, before being erupted at the surface or stalling in the lithosphere. The contribution of SCLM-derived volatiles to the SFB plume can therefore be estimated using differences in halogen and noble gas signatures between the Udachnaya (metasomatised SCLM) and Obnazhennaya (SFB + metasomatised SCLM) xenoliths.

Assuming that the melt residues in the Obnazhennaya lithosphere had a starting composition similar to the SFB plume (12.7R_A and mantle-like Br/Cl and I/Cl)[24,25] then the amount of assimilation from the SCLM (Udachnaya) can be estimated from the extent of mixing between the two sources (Fig. 2, 3, Supplementary Information). Comparing He, Br and I systematics between the SFB plume and the SCLM component represented by Udachnaya, requires that up to 70% of volatiles in Obnazhennaya be derived from the SCLM (Fig. 3a,b, Supplementary Fig. 2). Furthermore, any potential overprinting related to crustal assimilation affecting the halogen composition of the melt can be excluded as the rapid transport of xenoliths to the surface via kimberlite volcanism limits any potential interaction with the surrounding crust[26,27].

159 Taking the volume of Cl degassed as calculated from the SFB melt inclusions
160 (8.7×10^{15} kg), then the total fluxes of Br and I to the atmosphere are estimated to be
161 2.3×10^{13} kg and 9.6×10^{10} kg respectively. This calculation assumes the melt had
162 Br/Cl and I/Cl values similar to Obnazhennaya and considers that halogens are not
163 fractionated during degassing[28]. Explosive eruptions inject reactive HCl and HBr
164 gases into the lower stratosphere (~12-25 km) and deplete ozone levels, whereas
165 effusive eruptions lead to soluble HCl being washed-out prior to reaching the
166 stratosphere[24]. Considering only explosive events (20-30% of the SFB)[29], a ~75%
167 rate of stratospheric injection[30], and the amount of Cl measured within the SFB[31],
168 then the mass of Cl released to the stratosphere over the main eruptive phase of the
169 SFB (two thirds of the total eruptive volume over 300ky)[32] is the equivalent to 0.5-1.0
170 Pinatubo (1991-1992) eruptions, which caused a 15-20% reduction in global
171 ozone[33], every year for 300ky. Models of ozone depletion during the SFB eruption,
172 using estimated stratospheric HCl fluxes predict a 30-55% reduction in ozone over
173 the same eruptive timeframe[4]. These stratospheric HCl flux estimates are 5 times
174 lower than the predicted from the SFB melt inclusions (8.7×10^{15} kg)[31]. Furthermore,
175 these estimates do not take into account the consequences of Br degassing on
176 ozone depletion. The large release of Br to the stratosphere during the SFB, as
177 indicated by the high Br/Cl of the Siberian SCLM, likely further exacerbated ozone
178 depletion. Bromine has a much greater capacity for depleting ozone (~45× more
179 effective[24]) and could have reduced ozone levels by a further 20% during SFB
180 eruption. Although there are several uncertainties in the rate and magnitude of
181 volatile degassing during SFB magmatism, the scale of halogen degassing fluxes
182 presented here are sufficient to incur a near to total loss of global ozone during the
183 end-Permian crisis.

Melt inclusions within the SFB contain between 0.01-0.33 wt.% Cl[10,31], which is an order of magnitude higher than the maximum measured Cl concentrations in other LIPs[8,31]. Inclusions with high Cl concentrations are found to be equally enriched in other volatiles species such as fluorine (1.95 wt. %) and sulphur (0.51 wt. %)[31]. To create such high volatile contents within these melts, starting from a DMM-like composition, would require very low degree partial melting, or the assimilation of volatiles from another unknown reservoir. Low degrees partial melting can concentrate volatiles in the melt fraction, however the high Mg contents measured within the melt inclusions preclude low degree partial melting, suggesting that the assimilation of volatile-rich material is most likely cause of the high volatile contents in the SFB.

The composition of the Obnazhennaya xenoliths, assumed to represent plume melt residues, can be used to estimate the pre-eruptive SFB melt composition and establish if the SCLM is the potential source of the SFB volatile enrichment. Obnazhennaya xenoliths require ~30% melt extraction to account for the elevated $Fo_{>92}$ of the olivines[13] and therefore the Cl composition of this melt can be estimated using a batch melting model[34.] Experimentally determined partition coefficients for Cl between olivine ($D_{Cl}^{Ol/Melt} = 1.9\times10^{-2}$) and pyroxene ($D_{Cl}^{Pyx/Melt} = 1.5\times10^{-2}$) were used to calculate the Cl concentration of the melt at 1500°C, prior to eruption[35]. Using the range of Cl concentrations in the olivine and pyroxene minerals from Obnazhennaya xenoliths yield Cl concentrations of 0.1-0.2 wt.% in the melt. These estimates are considered upper limits given the potential for an unknown proportion of intact fluid inclusions to remain following crushing, thus Cl data based on stepped heating is likely to overestimate the Cl abundance within the minerals. However, it is notable

that the melt Cl estimates are consistent with previous values for the eruptive melt composition (0.01-0.33 wt.% Cl)[10,32] providing confidence in the assumptions we have made and confirming that the SFB melt was already enriched in Cl prior to eruption. These arguments therefore provide further (albeit indirect) support for a SCLM origin for the majority of halogens in SFB melts.

Implications for the end-Permian extinction

Ozone depletion during the end-Permian crisis is considered to have led to the decline in the dominant terrestrial plant species at the time, followed by the rapid expansion of opportunistic lycopsids[36]. The global distribution of preserved microspores from these emerging lycopsides exhibit features indicative of a failure in the normal development process of the spores. The global dispersion of these mutagenic spores suggest that this was a reaction to global stress factors, unlikely to be related to changes in global temperature from the release of gases such as SO_2 and CO_2 during SFB emplacement[4]. Experiments on the effects of end-Permian UV-B regimes on modern conifers led to a fivefold increases in the occurrence of mutagenic malformations, and complete sterilisation[37]. This would have caused widespread deforestation and the collapse of the terrestrial biosphere, indicating ozone depletion was a major contributing factor in the end-Permian mass extinction event[4,37].

The peak occurrence of mutagenic spores occurs prior to the rapid negative shift in $\delta^{13}C$ in end-Permian carbonates attributed to the extinction of calcified marine life[36].

232 The $\delta^{13}C$ excursions coincide with a change from predominantly extrusive to
233 intrusive eruptions of the Siberian LIP[1]. The emplacement of sills into volatile rich
234 sediments was considered to have released vast quantities of volatiles including CO_2
235 and halocarbons gases to the atmosphere leading to rapid climate change and
236 ozone depletion[1,5]. However, from the palynological evidence[36] it is clear that a
237 reduction in terrestrial biodiversity was occurring prior to the onset of marine
238 extinction. Furthermore, evidence for reduced sedimentation rates prior to and up to
239 the PTB, indicates that there was global eustatic sea-level regression potentially
240 caused by falling global temperatures and the onset of glaciation[38]. The rapid fall in
241 temperatures has been linked to the emission of SO_2 to the atmosphere during the
242 eruptive phase of the SFB[7].

243

244 The concurrent timing of the eruptive phase of the SFB and the palynological
245 evidence for ozone depletion is not consistent with the idea of sedimentary brines
246 degassing during later intrusive phases of igneous activity being the primary source
247 of halogens causing ozone destruction. As we have shown in this study the majority
248 of halogens in the SFB were added during plume-lithosphere interaction followed by
249 their subsequent release to the atmosphere during explosive eruptions. Sulphur
250 enrichments, co-existing with halogens in SFB[31], may also have been derived from
251 the SCLM (Fig. 4c). Evidence for terrestrial species decline prior to PTB therefore
252 suggests that the release of halogens and gaseous sulphur species, and the
253 subsequent decline in ozone and global temperatures respectively were the
254 predominant factors in initiating the end-Permian mass extinction. The change in
255 eruptive phase from explosive to intrusive may have played a role in extending the
256 extinction from a mainly terrestrial phenomenon to a global extinction event.

Subducted origin of volatiles in the Siberian lithosphere

The high concentrations of halogens in the Udachnaya xenoliths indicate the Siberian SCLM has been enriched in volatiles by metasomatic processes. Udachnaya xenoliths have Br/Cl and I/Cl similar to fluids trapped within minerals in the altered oceanic crust (AOC), suggesting that the metasomatism of the Siberian SCLM was potentially driven by subduction derived fluids (Fig. 2)[39]. Combined with the noble gases (Fig. 3; Supplementary Fig. 3 and 4) the Udachnaya xenoliths show an evolution from seawater-like $^{3}He/^{4}He$, Br/Cl and I/Cl values, to values with increasingly radiogenic $^{3}He/^{4}He$ and enriched Br/Cl and I/Cl (Fig. 3), further suggesting that the metasomatic fluid originated as seawater but subsequently evolved, during subduction or within the SCLM, due to halogen fractionation and the production of ^{4}He from U-Th decay[18]. Eclogite xenoliths from the Udachnaya kimberlite exhibit $\delta^{18}O$ up to +7.7%[40], outwith the normal mantle range (+5.4 ± 0.2%)[41] indicating that they originated as oceanic crust that underwent low temperature alteration[40]. Eclogites formed from the subduction of oceanic crust have been shown to retain the halogen and oxygen isotopic signature of the oceanic crust protolith during metamorphism, providing a mechanism for the delivery of subduction-derived halogens to the Siberian SCLM[42,43].

As we have shown in this study, up to 70% of the volatile content of the Siberian plume originated from assimilation of metasomatised lithospheric material. The composition of the SCLM therefore plays an integral role in controlling the volatile content of LIPs, and as such the overall effect they have on the global environment.

Based on the evolution of the Br/Cl, I/Cl and $^{3}He/^{4}He$ of the xenoliths from seawtaer to AOC-like values, coupled with the AOC-like $\delta^{18}O$ within eclogites xenoliths from Udachnaya, its appears that the origin of the Siberian SCLM volatiles is from the subduction of a seawater derived component within the AOC. Enrichment of seawater-derived volatiles in the Siberian SCLM provided the plume with an abundant supply of halogens, which were released to the atmosphere during eruption and resulted in globally extensive reductions in ozone levels and the decline of the biosphere. The SCLM is also a major repository for other subducted volatile species including sulphur and carbon[44,45], which can also contribute to environmental degradation during plume-lithosphere interaction and LIP emplacement[7]. The SCLM can therefore act as a repository of subducted volatile that can periodically be mobilised and released to the Earth's surface and atmosphere during deep-seated melting and volcanism leading to devastating impacts on the global environment.

References

1 Burgess, S., Muirhead, J. & Bowring, S. Initial pulse of Siberian Traps sills as the trigger of the end-Permian mass extinction. *Nature Communications* **8** (2017).

2 Wignall, P. B. Large igneous provinces and mass extinctions. *Earth-science reviews* **53**, 1-33 (2001).

3 Erwin, D. H., Bowring, S. A. & Yugan, J. End-Permian mass extinctions: a review. *Special Paper - Geological Soceity of America*, 363-384 (2002).

4 Beerling, D. J., Harfoot, M., Lomax, B. & Pyle, J. A. The stability of the stratospheric ozone layer during the end-Permian eruption of the Siberian Traps. *Philosophical Transactions of the Royal Society of London A: Mathematical, Physical and Engineering Sciences* **365**, 1843-1866 (2007).

5 Svensen, H. *et al.* Siberian gas venting and the end-Permian environmental crisis. *Earth and Planetary Science Letters* **277**, 490-500 (2009).

6 Grard, A., Francois, L., Dessert, C., Dupré, B. & Godderis, Y. Basaltic volcanism and mass extinction at the Permo-Triassic boundary: environmental impact and modeling of the global carbon cycle. *Earth and Planetary Science Letters* **234**, 207-221 (2005).

7 Guex, J. *et al.* Thermal erosion of cratonic lithosphere as a potential trigger for mass-extinction. *Scientific reports* **6**, 23168 (2016).

8 Self, S., Widdowson, M., Thordarson, T. & Jay, A. E. Volatile fluxes during flood basalt eruptions and potential effects on the global environment: A Deccan perspective. *Earth and Planetary Science Letters* **248**, 518-532 (2006).

9 Sobolev, A., Sobolev, S., Kuzmin, D., Malitch, K. & Petrunin, A. Siberian meimechites: origin and relation to flood basalts and kimberlites. *Russian Geology and Geophysics* **50**, 999-1033 (2009).

10 Sobolev, S. V. *et al.* Linking mantle plumes, large igneous provinces and environmental catastrophes. *Nature* **477**, 312 (2011).

11 Reichow, M. K. *et al.* $^{40}Ar/^{39}Ar$ dates from the West Siberian Basin: Siberian flood basalt province doubled. *Science* **296**, 1846-1849 (2002).

12 Ivanov, A. V. *et al.* Siberian Traps large igneous province: Evidence for two flood basalt pulses around the Permo-Triassic boundary and in the Middle Triassic, and contemporaneous granitic magmatism. *Earth-Science Reviews* **122**, 58-76 (2013).

13 Pernet-Fisher, J. *et al.* Plume impingement on the Siberian SCLM: Evidence from Re–Os isotope systematics. *Lithos* **218**, 141-154 (2015).

14 Walker, R., Carlson, R., Shirey, S. & Boyd, F. Os, Sr, Nd, and Pb isotope systematics of southern African peridotite xenoliths: implications for the chemical evolution of subcontinental mantle. *Geochimica et Cosmochimica Acta* **53**, 1583-1595 (1989).

15 McDonough, W. Constraints on the composition of the continental lithospheric mantle. *Earth and Planetary Science Letters* **101**, 1-18 (1990).

16 Taylor, L. A., Milledge, H. J., Bulanova, G. P., Snyder, G. A. & Keller, R. A. Metasomatic eclogitic diamond growth: evidence from multiple diamond inclusions. *International Geology Review* **40**, 663-676 (1998).

17 Howarth, G. H. *et al.* Superplume metasomatism: evidence from Siberian mantle xenoliths. *Lithos* **184**, 209-224 (2014).

18 Barry, P. H. *et al.* Helium isotopic evidence for modification of the cratonic lithosphere during the Permo-Triassic Siberian flood basalt event. *Lithos* **216**, 73-80 (2015).

19 Griffin, W., Fisher, N., Friedman, J., O'Reilly, S. Y., & Ryan, C. (2002). Cr-pyrope garnets in the lithospheric mantle 2. Compositional populations and their distribution in time and space. *Geochemistry, Geophysics, Geosystems*, 3(12), 1-35.

20 Kendrick, M. *et al.* Seawater cycled throughout Earth's mantle in partially serpentinized lithosphere. *Nature Geoscience* **10**, 222-228 (2017).

21 Burgess, R., Layzelle, E., Turner, G. & Harris, J. Constraints on the age and halogen composition of mantle fluids in Siberian coated diamonds. *Earth and Planetary Science Letters* **197**, 193-203 (2002).

22 Johnston, D. A. Volcanic contribution of chlorine to the stratosphere: more significant to ozone than previously estimated? *Science* **209**, 491-493 (1980).

23 Daniel, J., Solomon, S., Portmann, R. & Garcia, R. Stratospheric ozone destruction: The importance of bromine relative to chlorine. *Journal of Geophysical Research: Atmospheres* **104**, 23871-23880 (1999).

24 Kendrick, M. A., Kamenetsky, V. S., Phillips, D. & Honda, M. Halogen systematics

(Cl, Br, I) in mid-ocean ridge basalts: a Macquarie Island case study. *Geochimica et Cosmochimica Acta* **81**, 82-93 (2012).

25 Basu, Asish R., et al. High-^{3}He plume origin and temporal-spatial evolution of the Siberian flood basalts. *Science* **269** (5225), 822-825 (1995).

26 Kelley, S. & Wartho, J. Rapid kimberlite ascent and the significance of Ar-Ar ages in xenolith phlogopites. *Science* **289**, 609-611 (2000).

27 Alexeev, S. *et al.* Isotopic composition (H, O, Cl, Sr) of ground brines of the Siberian Platform. *Russian Geology and Geophysics* **48**, 225-236 (2007).

28 Black, B. A., Elkins-Tanton, L. T., Rowe, M. C. & Peate, I. U. Magnitude and consequences of volatile release from the Siberian Traps. *Earth and Planetary Science Letters* **317**, 363-373 (2012).

29 Aiuppa, A. *et al.* Emission of bromine and iodine from Mount Etna volcano. *Geochemistry, Geophysics, Geosystems* **6** (2005).

30 Ross, P.-S. *et al.* Mafic volcaniclastic deposits in flood basalt provinces: a review. *Journal of Volcanology and Geothermal Research* **145**, 281-314 (2005).

31 Millard, G. A., T. A. Mather, D. M. Pyle, William I. Rose, and B. Thornton. "Halogen emissions from a small volcanic eruption: Modeling the peak concentrations, dispersion, and volcanically induced ozone loss in the stratosphere." *Geophysical*

Research Letters **33(19)** (2006).

32 Burgess, S. D., & Bowring, S. A. High-precision geochronology confirms voluminous magmatism before, during, and after Earth's most severe extinction. *Science Advances*, 1(7) (2015).

33 Westrich, H. R., & Gerlach, T. M. Magmatic gas source for the stratospheric SO_2 cloud from the June 15, 1991, eruption of Mount Pinatubo. *Geology*, **20**(10), 867-870 (1992).

34 Shaw, D. M. Trace elements in magmas: a theoretical treatment, Cambridge University Press (2006).

35 Joachim, B. *et al.* Experimental partitioning of F and Cl between olivine, orthopyroxene and silicate melt at Earth's mantle conditions. *Chemical Geology* **416**, 65-78 (2015).

36 Visscher, H., Looy, C. V., Collinson, M. E., Brinkhuis, H., Van Konijnenburg-Van Cittert, J. H., Kürschner, W. M., & Sephton, M. A. Environmental mutagenesis during the end-Permian ecological crisis. *Proceedings of the National Academy of Sciences of the United States of America,* 101(35), 12952-12956 (2004).

37 Benca, Jeffrey P., Ivo AP Duijnstee, and Cindy V. Looy. "UV-B–induced forest sterility: Implications of ozone shield failure in Earth's largest extinction." *Science advances* **4.2** (2018)

38 Baresel, B., Bucher, H., Bagherpour, B., Brosse, M., Guodun, K., & Schaltegger, U. Timing of global regression and microbial bloom linked with the Permian-Triassic boundary mass extinction: implications for driving mechanisms. *Scientific Reports*, **7**, 43630 (2017).

39 Chavrit, D. *et al.* The contribution of hydrothermally altered ocean crust to the mantle halogen and noble gas cycles. *Geochimica et Cosmochimica Acta* **183**, 106-124 (2016).

40 Jacob, D., Jagoutz, E., Lowry, D., Mattey, D. & Kudrjavtseva, G. Diamondiferous eclogites from Siberia: remnants of Archean oceanic crust. *Geochimica et Cosmochimica Acta* **58**, 5191-5207 (1994).

41 Eiler, J. M. Oxygen isotope variations of basaltic lavas and upper mantle rocks. *Reviews in mineralogy and geochemistry* **43**, 319-364 (2001).

42 Svensen, H., Jamtveit, B., Banks, D. A. & Austrheim, H. Halogen contents of eclogite facies fluid inclusions and minerals: Caledonides, western Norway. *Journal of Metamorphic Geology* **19**, 165-178 (2001).

43 Philippot, P., Agrinier, P., & Scambelluri, M. Chlorine cycling during subduction of altered oceanic crust. *Earth and Planetary Science Letters*, **161**(1-4), 33-44 (1998).

44 Callegaro, S. *et al.* Microanalyses link sulfur from large igneous provinces and Mesozoic mass extinctions. *Geology* **42**, 895–898 (2014).

45 Foley, S.F. and Fischer, T.P., An essential role for continental rifts and lithosphere in the deep carbon cycle. *Nature Geoscience*, ***10***(12), 897-902 (2017)

46 Muramatsu, Y. *et al.* Halogen concentrations in pore waters and sediments of the Nankai Trough, Japan: Implications for the origin of gas hydrates. *Applied Geochemistry* **22**, 534-556 (2007).

Acknowledgments

This work is dedicated to L. A. T, who passed away in 2017. L. A. T. devoted his life to science and teaching, serving as an excellent mentor to P. H. B. during his time at University of Tennessee. This work was financially supported though a NERC studentship NE/J500057/1 (to M. W. B.) and a NERC (NE/M000427/1) and ERC (ERC-267692 NOBLE) grant to C. J. B. and R. B. P. H. B. was funded by an NSF fellowship (EAR-114455) to investigate the geochemical signatures in these samples.

Author contributions

M. W. B, P. H. B and R. B conceived the project and prepared the initial manuscript. L.A.T provided the samples and M. W. B and R. B performed the analysis. All authors contributed to data analysis and preparation of the final manuscript.

Competing financial interests

The authors declare no competing financial interests**.**

Figure Captions

Figure 1. Halogen and K abundances in Udachnaya and Obnazhennaya xenoliths. Abundances of (a) Br, (b) I and (c) K plotted against Cl showing the enrichment of Br and I within the Siberian SCLM relative to the MORB/OIB mantle source and seawater[24]. Crushing ("crush") data are shown by open symbols and stepped-heating ("melt") by closed symbols. Errors bars are consistently covered by symbol. Uncertainties are presented at 1σ.

Figure 2. Halogen composition of the Siberian SCLM. Br/Cl versus I/Cl (a) crushing and (b) step heating of the Udachnaya and Obnazhennaya xenoliths. Xenoliths show a range of halogen compositions which overlap the range of Br/Cl and I/Cl observed in altered oceanic crust (AOC fluids) and eclogites. Seawater evaporation trend (SET) is shown, indicating that sedimentary brines cannot be responsible for the halogen signature of the xenoliths. Br/Cl and I/Cl results from halogen fractionation (black arrows) of AOC fluids (green star). Seawater, marine

pore fluids and MORB/OIB compositions are shown for reference[24,46]. Figure symbols are the same as in Figure 1. Uncertainties are 1σ.

Figure 3. Helium isotopes and halogen systematics. $^{3}He/^{4}He$ versus **(a)** I/Cl and **(b)** Br/Cl from crushed release of Udachnaya and Obnazhennaya xenoliths. Udachnaya has $^{3}He/^{4}He$, Br/Cl and I/Cl, which range from values similar to seawater (blue star) towards higher Br/Cl and I/Cl and lower $^{3}He/^{4}He$ characteristic subduction modified seawater. Obnazhennaya has higher $^{3}He/^{4}He$ ranging from Udachnaya-like towards OIB-like values, from the influx of plumes melts. Mixing lines [r = $(^{4}He/Cl)_{plume}$ /$(^{4}He/Cl)_{SCLM}$] shown between a hypothetical SCLM component (black diamond, intercept through the data) and plume melts with the relative percentage of SCLM assimilation shown. Figure symbols are same as used in Figure 1. Uncertainties are 1σ.

Figure 4. Schematic of plume-lithosphere interaction within the Siberian craton. a) SCLM is composed partly of metasomatised peridotite from addition of subducted volatiles, which potentially seeds diamond formation. b) Intermittent influence of the Siberian plume drives kimberlite volcanism c) Plume melt impinges on the lithosphere, incorporating volatile rich SCLM material. Halogens released to the atmosphere during explosive SFB eruptions leading to the extensive ozone depletion. d) Plume retreats leaving a much-reduced SCLM with veins of melt residue, followed by a second period of kimberlitic volcanism, transporting melt residues and SCLM material to the surface.

Methods

Neutron irradiation noble gas mass spectrometry (NI-NGMS)

Olivine and clinopyroxene mineral separates from Udachnaya and Obnazhennaya peridotite xenoliths were selected for heavy halogen (Cl, Br and I) and K analysis using neutron-irradiated noble gas mass spectrometry (NI-NGMS)[47-52]. Samples weighing between 0.015 and 0.062 g were first cleaned with deionised water in an ultrasonic bath for 20 minutes, followed by a further 5 minutes in acetone. Samples were then dried under a heat lamp at 100°C, wrapped in Al foil and sealed in evacuated fused-silica tubes together with Hb3gr, scapolite and Shallowater meteorite standards to monitor noble gas proxy production from K and halogens[51].

Samples were irradiated in the GRICIT (MN2014b) facilities of the TRIGA Reactor, Oregon State University for a few hours each day between 22/04/2014 and 01/07/2014 giving a total irradiation time of 205 hours. Irradiation details and monitor values for this irradiation have been reported previously[51].

Noble gas proxy isotopes ($^{38}Ar_{Cl}$, $^{80}Kr_{Br}$, $^{128}Xe_{I}$ and $^{39}Ar_{K}$) formed during irradiation as well as natural Ar, Kr and Xe isotopes were measured on the MS1 mass spectrometer[52]. A subset of samples and repeat analyses were also performed on a Thermo Fisher Scientific ARGUS VI mass spectrometer[51]. Noble gases were firstly extracted from trapped fluid inclusions by loading samples into hand-operated

543 modified Nupro® valve crushers[53] (MS1 mass spectrometer). For bulk sample
544 analysis, powders from crushing analyses were loaded into in a tantalum resistance
545 furnace (MS1) and step heated using four temperature steps of 600°C, 1000°C,
546 1400°C and 1600°C to release halogens contained within the mineral matrix.
547 Halogens from four samples (UV33, UV88, UV357 and O129-74) were extracted
548 using a 10.6 μm wavelength CO_2 laser (Teledyne CETAC Fusions CO_2 – ARGUS
549 VI). In order to test that both extraction methods gave the similar results, sample
550 O97-12 was analysed using both the furnace and laser, Br/Cl and I/Cl varied by less
551 than 20% and 35% respectively between laser and furnace extraction suggesting
552 halogens were released in similar proportions using both extraction methods.
553 Halogens abundances were then calculated using the well-defined conversion
554 standards with known halogen concentrations (Hb3gr, scapolite and Shallowater
555 meteorite)[50,51], which monitor the efficiency of noble gas production through thermal
556 and epithermal neutron reactions.

557

558 Air calibrations and blanks were analysed daily to check the sensitivity and
559 background of the spectrometers, with maximum furnace blank values at 1600°C on
560 the MS1 being 1.65×10^{-10} cm^3 STP ^{40}Ar, 2.92×10^{-13} cm^3 STP ^{84}Kr and 3.54×10^{-14}
561 STP cm^3 ^{132}Xe and ARGUS VI blanks being 5.76×10^{-12} cm^3 STP ^{40}Ar and $1.41 \times$
562 10^{-15} cm^3 STP ^{132}Xe, with Kr blanks below detection limit. Noble gas purification
563 analytical procedures for the MS1 and ARGUS VI mass spectrometers as well as the
564 data reduction procedures have been documented previously[52,5é]. External precision
565 is reported at 3% (1σ) for Cl and 7% (1σ) for Br and I determinations.

566

Data availability

All data pertaining to this study is presented in the paper and the supplementary information. Correspondence and requests for materials should be addressed to the corresponding author.

Method References

47 Merrihue, C. & Turner, G. Potassium-argon dating by activation with fast neutrons. *Journal of Geophysical Research* 71, 2852-2857 (1966).

48 Böhlke, J. & Irwin, J. Laser microprobe analyses of Cl, Br, I, and K in fluid inclusions: Implications for sources of salinity in some ancient hydrothermal fluids. *Geochimica et Cosmochimica Acta* 56, 203-225 (1992).

49 Johnson, L., Burgess, R., Turner, G., Milledge, H. & Harris, J. Noble gas and halogen geochemistry of mantle fluids: comparison of African and Canadian diamonds. *Geochimica et Cosmochimica Acta* 64, 717-732 (2000).

50 Kendrick, M. A. High precision Cl, Br and I determinations in mineral standards using the noble gas method. *Chemical Geology* 292, 116-126 (2012).

51 Ruzié-Hamilton, L. et al. Determination of halogen abundances in terrestrial and extraterrestrial samples by the analysis of noble gases produced by neutron irradiation. *Chemical Geology* 437, 77-87 (2016).

52 Broadley, M. W., Ballentine, C. J., Chavrit, D., Dallai, L. & Burgess, R. Sedimentary halogens and noble gases within Western Antarctic xenoliths: Implications of extensive volatile recycling to the sub continental lithospheric mantle. *Geochimica et Cosmochimica Acta* 176, 139-156 (2016).

53 Stuart, F. & Turner, G. The abundance and isotopic composition of the noble gases in ancient fluids. *Chemical Geology: Isotope Geoscience section* 101, 97-109 (1992).

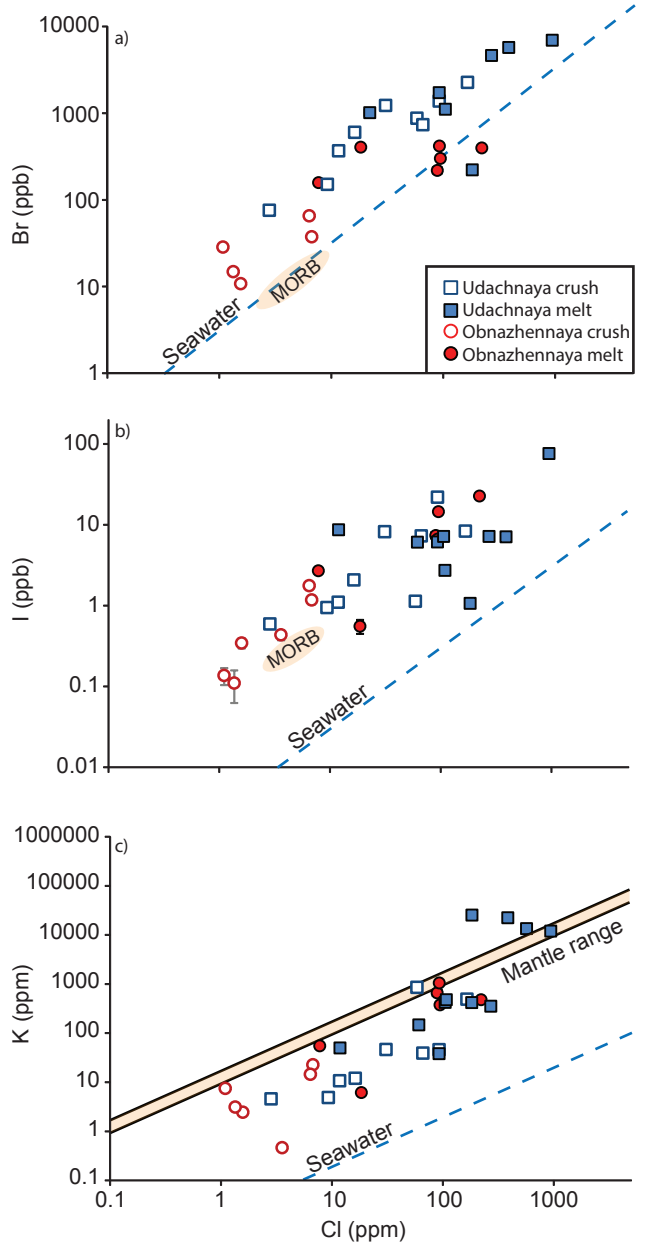
a)
Br (ppb)
10000
1000
100
10
1
Seawater
MORB
Udachnaya crush
Udachnaya melt
Obnazhennaya crush
Obnazhennaya melt
b)
I (ppb)
100
10
1
0.1
0.01
MORB
Seawater
c)
K (ppm)
1000000
100000
10000
1000
100
10
1
0.1
Mantle range
Seawater
0.1
1
10
100
1000
Cl (ppm)

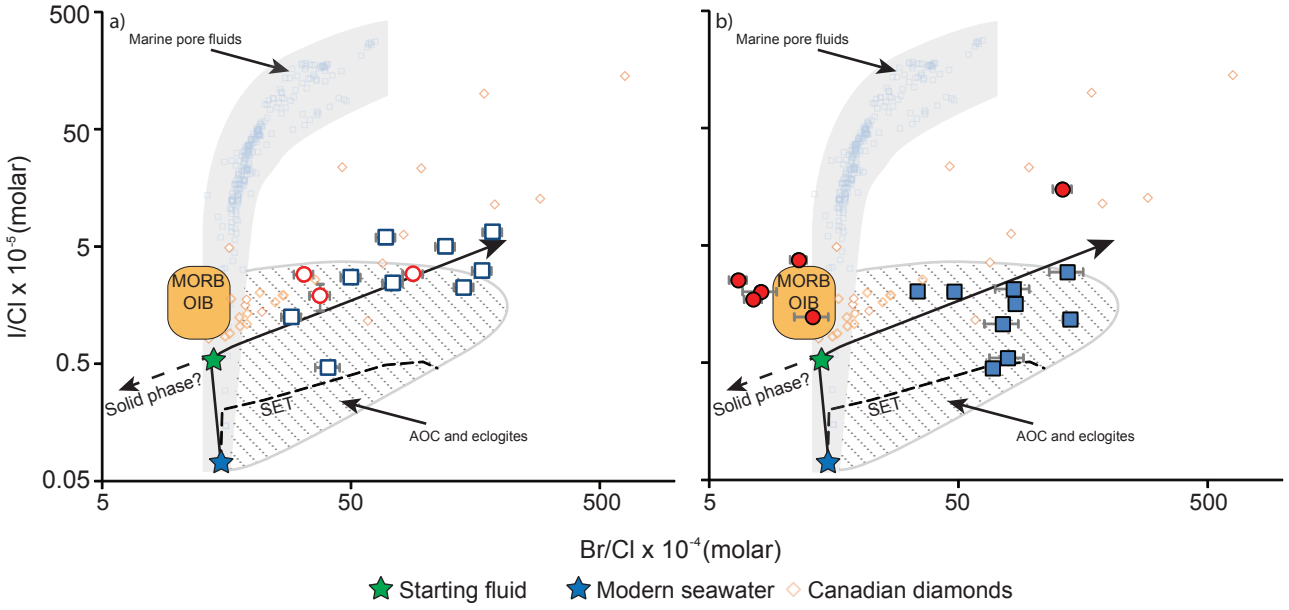
a)
b)
Marine pore fluids
MORB
OIB
Solid phase?
SET
AOC and eclogites
I/Cl x 10^{-5}(molar)
Br/Cl x 10^{-4}(molar)
500
50
5
0.5
0.05
Starting fluid
Modern seawater
Canadian diamonds

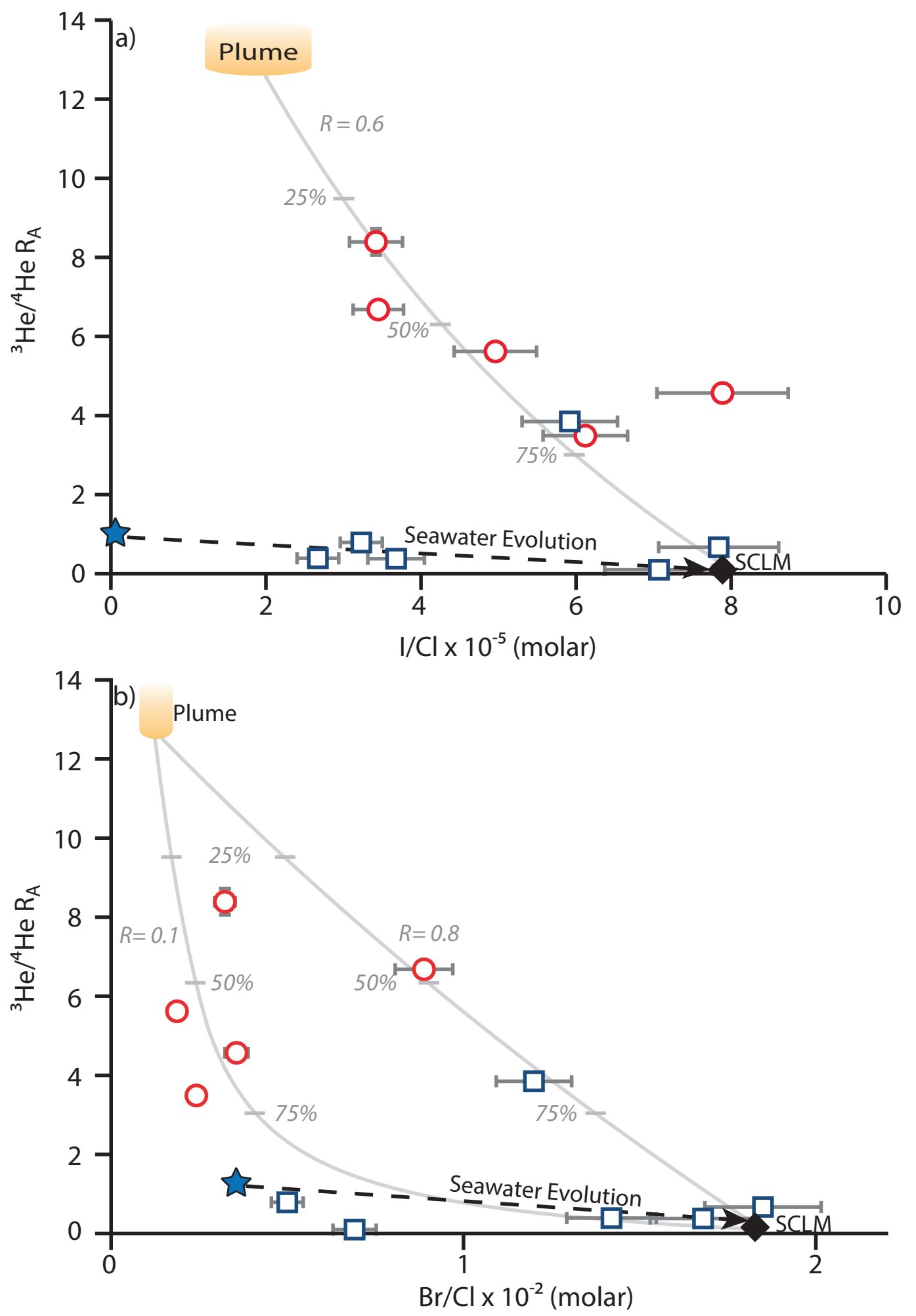
a)
Plume
R = 0.6
25%
50%
75%
Seawater Evolution
SCLM
$^3He/^4He\ R_A$
I/Cl x 10^{-5} (molar)
b)
Plume
25%
R= 0.1
R= 0.8
50%
50%
75%
75%
Seawater Evolution
SCLM
$^3He/^4He\ R_A$
Br/Cl x 10^{-2} (molar)

> 360 Ma Metasomatic episodes

a)

0 km

Continental Crust

SCLM

100km

graphite

diamond

Subduction metasomatism
and diamond formation

200 km

Asthenosphere

250 km

AOC dehydration

~ 360 Ma Eruption of Udachnaya

b)

Continental Crust

SCLM

Incorporation of diamonds
and SCLM xenoliths

graphite

diamond

Pulsed kimberlite eruption
driven by deep seated
heat source

~ 250 Ma Eruption of Siberian Flood Basalts

c)

HCl

S?

HBr

Volatile degassing
and depletion of ozone

HBr

HCl

S?

0 km

Continental Crust

SCLM

Percolating plume melts

100km

graphite

diamond

200 km

250 km

Assimilation of metasomatised
SCLM into rising melts

~ 160 Ma Eruption of Obnazhennaya

d)

Continental Crust

SCLM

Incorporation of
plume melt residues

Lithosphere eroded by plume

Decreasing plume
influence

Incorporation of plume melt residue
and SCLM xenoliths in Obnazhennaya